Carrier multiplication in semiconductor nanocrystals via intraband optical transitions involving virtual biexciton states

Valery I. Rupasov*
ALTAIR Center LLC, Shrewsbury, Massachusetts 01545, USA
and Landau Institute for Theoretical Physics, 117940 Moscow, Russia

Victor I. Klimov†
Chemistry Division, Los Alamos National Laboratory, Los Alamos, New Mexico 87545, USA
(Received 27 June 2007; published 25 September 2007)

We propose and analyze a physical mechanism for photogeneration of multiexcitons by single photons (carrier multiplication) in semiconductor nanocrystals, which involves intraband optical transitions within the manifold of biexciton states. In this mechanism, a virtual biexciton is generated from nanocrystal vacuum by the Coulomb interaction between two valence-band electrons, which results in their transfer to the conduction band. The virtual biexciton is then converted into a real, energy-conserving biexciton by photon absorption on an intraband optical transition. The proposed mechanism is inactive in bulk semiconductors as momentum conservation suppresses intraband transitions. However, it becomes highly efficient in the case of zero-dimensional nanocrystals, where quantum confinement results in relaxation of momentum conservation, which is accompanied by the development of strong intraband absorption. Our calculations show that the efficiency of the carrier multiplication channel mediated by intraband optical transitions can be comparable to or even greater than that for impact-ionization-like processes mediated by interband transitions.

DOI: 10.1103/PhysRevB.76.125321 PACS number(s): 78.67.Bf, 73.21.La, 78.47.+p

I. INTRODUCTION

Carrier multiplication (CM) is a process in which absorption of a single photon produces not just one but multiple electron-hole (*e-h*) pairs (excitons). CM can benefit a number of technologies, especially photovoltaics and photocatalysis. In bulk semiconductors, CM is typically explained by impact ionization.[1] In this process, a conduction-band electron or a valence-band hole of sufficiently high energy interacts with a valence-band electron promoting it across the energy gap (E_g). An important characteristic of CM is the *e-h* pair creation energy (ε) defined as the energy lost by the ionizing particle in a single *e-h* pair creation event. On the basis of energy conservation, the minimal value of ε is E_g. However, because of restrictions imposed by momentum conservation and significant phonon losses, the values of ε measured for bulk semiconductors significantly exceed this energy-conservation-defined limit. In particular, ε is approximately $3E_g$ for wide-gap semiconductors and even greater for narrow-gap materials.[2,3]

Recent experimental studies of zero-dimensional (0D) semiconductor nanocrystals[4–6] (NCs) indicate that in these structures, ε approaches its ultimate limit of E_g, which results in extremely high CM efficiencies.[6] The mechanism for this enhancement is not well understood. For example, Zunger and co-workers adopted a traditional impact-ionization model for treating CM in NCs.[7,8] On the other hand, recent calculations by Allan and Delerue[9] indicate that impact ionization is not enhanced by quantum confinement, suggesting the existence of either additional or alternative mechanisms for CM in NCs.

Two such mechanisms have been discussed by Efros and co-workers[5,10] and Schaller *et al.*[11] Their common motif is that CM occurs via direct Coulomb coupling of a single-exciton state, generated in a NC via an interband transition, to a biexciton state (corresponding matrix element U_{II} is the same as in the impact-ionization models). In Ref. 11, this process was treated using second-order perturbation theory as a transition via intermediate virtual single-exciton states, while Ref. 10 utilized a time-dependent density-matrix approach. In the limit of weak Coulomb coupling ($U_{II} < \Gamma_{xx}$; Γ_{xx} is the biexciton dephasing rate), both models lead to a similar result for the ratio of the biexciton (N_{xx}) to the single-exciton (N_x) populations. Specifically, in the case of a single intermediate exciton state (dephasing rate Γ_x) coupled to a single biexciton state, $N_{xx}/N_x = |U_{II}|^2/(\Gamma_x\Gamma_{xx})$. This expression shows that N_{xx}/N_x can be greater than unity only if $U_{II} > \Gamma_x$, which was regarded as a necessary condition for efficient CM in Ref. 10. However, as was pointed out in Ref. 11, the available experimental data indicate that Coulomb coupling in NCs is likely smaller than Γ_x. Therefore, it was suggested that an important factor contributing to the high efficiency of CM in NCs is a large density of biexciton states (g_{xx}), which can greatly exceed that of single-exciton states (g_x) of similar energies.[11] Recent pseudopotential calculations[8] indeed indicate fast increase in the g_{xx}-to-g_x ratio with increasing energy above the lowest biexciton resonance.

In this paper, we use second-order perturbation theory to analyze an unexplored aspect of the direct biexciton photogeneration model associated with the possibility of two different time orderings of the interaction terms responsible for photoexcitation and the Coulomb interaction. One time ordering, considered in Ref. 11, involves first *interband* optical excitation of an intermediate exciton state (virtual exciton), which is then converted into a final real biexciton via the impact-ionization term, H_{II}, of the Coulomb interaction (Fig. 1; left of the thick gray arrow). However, another possibility

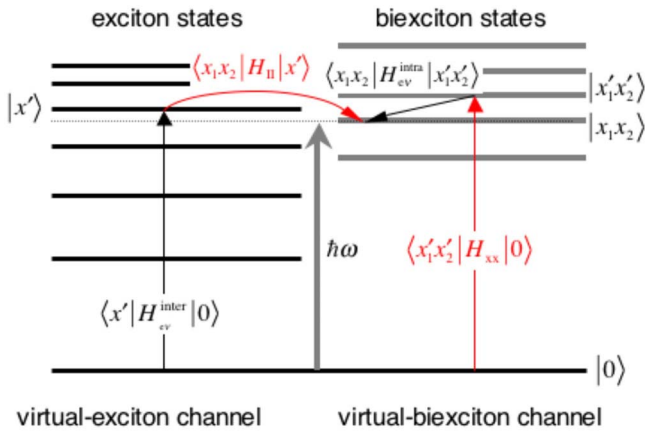

FIG. 1. (Color online) Direct photogeneration of a biexciton from vacuum, $|0\rangle$, via intermediate single-exciton (on the left) or intermediate biexciton (on the right) states. The final biexciton state $|x_1x_2\rangle$ is in resonance with the absorbed photon, while intermediate (virtual) single-exciton $|x'\rangle$ and biexciton $|x'_1x'_2\rangle$ states can be off resonance (energy conservation is not required for virtual processes). The order of processes involving electron-photon and carrier-carrier Coulomb interactions for the virtual biexciton channel is reversed with respect to that for the virtual exciton channel. H_{II} and H_{xx} are the components of the Coulomb-interaction operator responsible for impact-ionization and biexciton generation from vacuum, respectively. H_{ev}^{inter} and H_{ev}^{intra} are the operators of the electron-photon interaction responsible for the interband and intraband transitions, respectively.

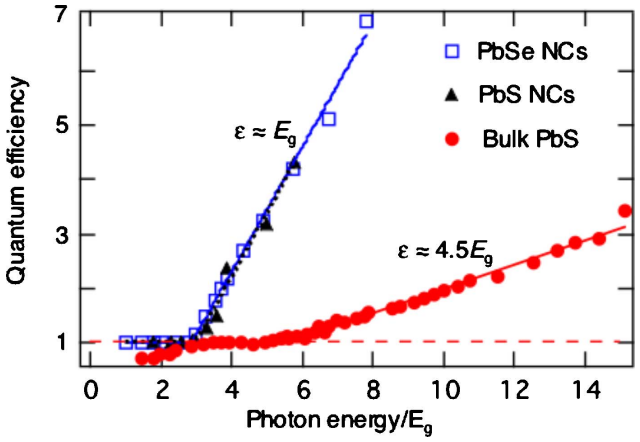

FIG. 2. (Color online) Spectral dependence of quantum efficiencies measured for bulk PbS (data from Ref. 13) as well as PbS and PbSe NCs (from Ref. 6).

is generation of an intermediate biexciton state (virtual biexciton) from NC vacuum via the Coulomb-interaction component H_{xx}, which involves transfer of two electrons from the valence to the conduction band (Fig. 1; right of the thick gray arrow); this intermediate biexciton state is then converted into a final real biexciton via an *intraband* optical transition initiated by the absorbed photon.

The time ordering in the virtual biexciton channel is similar to that in one of the two channels for the Raman process, in which an excitation of a quantum system with simultaneous emission of a Stokes photon precedes absorption of an incident photon.[12] Furthermore, as in the Raman process, the total probability amplitude of biexciton photogeneration is determined by contributions from both virtual exciton and virtual biexciton channels.

Using density-of-states arguments and taking into account the large strength of NC intraband transitions, we show that the CM rate for the mechanism involving intermediate biexciton states can approach the total photogeneration rate even for weak Coulomb coupling on the order of 1 meV. The overall spectral dependence of the CM efficiency calculated for PbSe NCs is consistent with that observed experimentally.[4–6,11] We also demonstrate that the CM rate for the virtual biexciton channel can be comparable to or higher than the CM rate for the channel involving virtual single-exciton states, suggesting that the proposed mechanism can provide a dominant contribution to the CM process in NCs.

An important feature of the process discussed here is that it is inactive in bulk materials because of translational-momentum conservation, which greatly reduces the efficiency of virtual intraband optical transitions. On the other hand, because of relaxation of momentum conservation, the proposed mechanism can become highly efficient in 0D nanostructures. The existence of this additional CM channel, which operates in parallel with impact-ionization-like processes[11] (and possibly even dominates them), may explain unusually high efficiencies of CM in NCs.

II. TWO PATHWAYS FOR DIRECT PHOTOGENERATION OF BIEXCITONS

Available experimental data indicate that CM in NCs does not follow the trends previously established for bulk semiconductors, which might be considered as a sign that this process occurs via different pathways in these two classes of materials. For example, Fig. 2 compares quantum efficiencies (Q) for conversion of photons into e-h pairs measured as a function of photon energy ($\hbar\omega$) for bulk PbS[13] as well as PbS and PbSe NCs.[6] This comparison indicates a considerably lower CM threshold in NCs ($\sim 3E_g$) than in the bulk ($\sim 5E_g$). The other difference is in the slope of the Q-vs-$\hbar\omega$ dependence, which provides a direct measure of the e-h pair creation energy: $\varepsilon = d(\hbar\omega)/dQ$. Based on the data in Fig. 2, $\varepsilon = 4.5E_g$ in bulk PbS, while it is $\sim E_g$ in PbS and PbSe NCs.

The e-h creation energy is normally calculated as a sum of E_g, the average kinetic energy of carriers following the impact-ionization event ($\langle E_K\rangle$), and the energy lost to phonons ($\langle E_{ph}\rangle$).[2,3] Since ε measured for NCs is close to E_g, it implies that both $\langle E_K\rangle$ and $\langle E_{ph}\rangle$ are approaching zero. The fact that $\langle E_K\rangle = 0$ can be attributed to relaxation of momentum conservation, while the zero value of $\langle E_{ph}\rangle$ indicates that CM in NCs occurs without measurable phonon losses. The latter is an important conclusion, which allows one to treat CM not as a competition between impact ionization and phonon-assisted relaxation (traditional approach used for bulk semiconductors) but as *direct* photogeneration of biexcitons via intermediate either single-exciton[11] or biexciton states (Fig. 1).

If we neglect the interference between different CM pathways, the total biexciton photogeneration rate W_2 can be presented as a sum of two rates $W_{2,x}$ and $W_{2,xx}$, which correspond, respectively, to the virtual exciton and the virtual biexciton channels: $W_2=W_{2,x}+W_{2,xx}$. The first of these pathways was analyzed in Ref. 11. Here, we will concentrate on the second pathway involving intermediate biexciton states. We will also perform a comparison of CM efficiencies for these two processes.

III. CARRIER MULTIPLICATION MEDIATED BY INTRABAND OPTICAL TRANSITIONS

An important feature of the virtual biexciton CM channel is that it is not efficient in bulk semiconductors. It involves the final virtual transition mediated by intraband absorption, while the latter process is suppressed in bulk materials by translational-momentum conservation. In bulk semiconductors, real intraband optical transitions are strictly forbidden by energy and translation-momentum conservation. The energy-conservation requirement is lifted in the case of virtual intraband transitions, which makes them nominally allowed. However, the restrictions imposed by momentum conservation alone greatly reduce the efficiency of these processes, which renders the virtual biexciton channel inactive in bulk materials. On the other hand, because of relaxation of momentum conservation, intraband transitions are strong in low-dimensional nanostructures, which can result in a significant efficiency of biexciton generation via intraband absorption. The existence of the CM channel, which is not active in bulk semiconductors but becomes greatly enhanced in 0D nanostructures, can, in principle, explain a significant enhancement in the CM efficiency in NCs.

The Coulomb-interaction term, which is involved in the virtual biexciton CM channel, describes scattering between two valence-band electrons accompanied by their transfer to the conduction band, and it can be presented as

$$H_{xx}=\frac{1}{4}\sum_{a_1a_2b_1b_2}[U_{b_1b_2}^{a_1a_2}c_{a_1}^{\dagger}c_{a_2}^{\dagger}d_{b_1}d_{b_2}+\text{H.c.}], \tag{1}$$

$$U_{b_1b_2}^{a_1a_2}=\int d\mathbf{r}_1d\mathbf{r}_2\Psi_{a_1}^{*}(\mathbf{r}_1)\Psi_{a_2}^{*}(\mathbf{r}_2)U_C(|\mathbf{r}_1-\mathbf{r}_2|)\times[\Psi_{b_1}(\mathbf{r}_2)\Psi_{b_2}(\mathbf{r}_1)-\Psi_{b_2}(\mathbf{r}_2)\Psi_{b_1}(\mathbf{r}_1)], \tag{2}$$

where $U_C=e^2/(\kappa|\mathbf{r}_1-\mathbf{r}_2|)$ is the Coulomb-interaction energy (e is the electron charge and κ is the dielectric permittivity of a NC), $c^{\dagger}$ (c) and $d^{\dagger}$ (d) are electron creation (annihilation) operators for the conduction and the valence bands, respectively, and Ψ is the electron wave function for the conduction (index a) or the valence (index b) bands. Application of the operator H_{xx} upon the NC vacuum state $|0\rangle$ creates two electrons in the conduction band and two holes in the valence band, i.e., a biexciton. Since energy is not conserved in this process, it does not contribute to transition rates calculated within first-order perturbation theory. However, its contribution is nonzero in second-order perturbation theory. In this case, the intermediate, virtual biexciton state $|x_1'x_2'\rangle$ generated from vacuum by the operator H_{xx} is converted into a real biexciton, $|x_1x_2\rangle$, by the intraband optical transition (Fig. 1; right of the thick gray arrow). This two-step process produces a final state with energy $E_{x_1x_2}$, which satisfies energy conservation ($E_{x_1x_2}=\hbar\omega$, where $\hbar\omega$ is the photon energy), and the corresponding rate can be calculated as

$$W_{2,xx}=\frac{2\pi}{\hbar}\sum_{x_1x_2}\left|\sum_{x_1'x_2'}\frac{\langle x_1x_2|H_{ev}^{\text{intra}}|x_1'x_2'\rangle\langle x_1'x_2'|H_{xx}|0\rangle}{E_{x_1'x_2'}}\right|^2, \tag{3}$$

where $E_{x_1'x_2'}$ is the energy of the intermediate biexciton states and H_{ev}^{intra} is the part of the electron-photon coupling operator responsible for intraband transitions, which changes the state of only one of four carriers comprising the intermediate biexciton state. The contribution to rate $W_{2,xx}$ from interband transitions is canceled by the analogous term with the reversed order of the operators H_{xx} and H_{ev}^{inter}. In the case of intraband transitions, the latter term vanishes because $H^{intra}|0\rangle=0$ (in the vacuum state, the valence band in fully occupied while the conduction band is completely empty), and hence, the resulting biexciton generation rate is *nonzero*. Further, because of the significant strength of intraband transitions in NCs[14] and a large number of intermediate and final biexciton states, the process described by Eq. (3) can be highly efficient despite its nonresonant character [the denominator in Eq. (3) is the energy of the intermediate biexciton state, which is at least $2E_g$].

IV. NUMERICAL ESTIMATES: LEAD SELENIDE NANOCRYSTALS

To estimate the CM efficiency for the virtual biexciton mechanism, we consider lead-salt NCs using the description of electronic states developed by Kang and Wise.[15] In this formalism, electronic states are characterized by parity (π), total angular momentum (j), and projection thereof (m); j is the sum of the orbital angular momentum (l) and the particle spin (s). The parities of the $2(2l+1)$-fold degenerate energy levels are $\pi=-(-1)^l$ in the conduction band and $\pi=(-1)^l$ in the valence band. The multivalley structure of lead salts leads to an additional fourfold degeneracy of each of the above electronic states (the intervalley coupling is small compared to transition linewidths and, therefore, is not expected to appreciably split this degeneracy).

The selection rules for dipole-allowed intraband transitions are $\Delta j=0,\pm1$, $\Delta m=0,\pm1$, and $\pi_1\pi_2=-1$.[15] Because of the requirement $\pi_1\pi_2=-1$, the operator H_{ev}^{intra} is odd. Since the Coulomb energy $U_C(|\mathbf{r}_1-\mathbf{r}_2|)$ is not modified under spatial inversion ($\mathbf{r}_1\rightarrow-\mathbf{r}_1$ and $\mathbf{r}_2\rightarrow-\mathbf{r}_2$), the matrix element $U_{b_1b_2}^{a_1a_2}$ is nonzero only for states that satisfy the condition $\pi_{c_1}\pi_{c_2}\pi_{d_1}\pi_{d_2}=+1$, which indicates that the operator H_{xx} is even. Finally, because the vacuum state of a NC is even, the final biexciton state $|x_1x_2\rangle$ generated by the product of operators H_{xx} and H_{ev}^{intra} is odd, and hence, the product of the parities of all four carriers in the final biexciton state must be -1.

Based on parity considerations, the energy onset for CM ($\hbar\omega_{\text{CM}}$) corresponds to the lowest-energy odd biexciton state.

Such a state comprises three $1S$ carriers ($l=0$) and one $1P$ carrier ($l=1$), and hence, $\hbar\omega_{\mathrm{CM}}=3E(1S)+E(1P)=2E_g+[E(1P)-E(1S)]$. Using the energies computed in the supporting information of Ref. 5, we obtain $\hbar\omega_{\mathrm{CM}}=2.25E_g$. This result indicates that, because of the selection rules, the CM threshold is higher than the $2E_g$ limit defined by energy conservation.

To estimate the rate $W_{2,xx}$, we replace the energy of the intermediate biexciton states $E_{x_1'x_2'}$ with $2E_g$ and approximate matrix elements of operators H_{xx} and H_{ev}^{intra} with their average values (U_{xx} and V_{intra}, respectively). By further performing the summation in Eq. (3) over the intermediate and the final biexciton states, we obtain

$$W_{2,xx}\approx\frac{2\pi}{\hbar}\left|\frac{g'_{xx}V_{\mathrm{intra}}U_{xx}}{2E_g}\right|^2 g_{xx}, \tag{4}$$

where g'_{xx} is number of the intermediate biexciton states, while g_{xx} is number of the final biexciton states with energy $E_{xx}=\hbar\omega$. We quantify the CM efficiency in terms of the ratio of the biexciton generation rate ($W_{2,xx}$) and the total photogeneration rate (W): $f=W_{2,xx}/W$. The rate W can be calculated using first-order perturbation theory: $W\approx(2\pi/\hbar)|V_{\mathrm{inter}}|^2 g_x$, where g_x is the number of single-exciton resonances at energy $\hbar\omega$ and V_{inter} is the average matrix element of the interband transitions. Finally, we obtain

$$f\approx\left(g'_{xx}\frac{V_{\mathrm{intra}}}{V_{\mathrm{inter}}}\right)^2\left(\frac{U_{xx}}{2E_g}\right)^2\frac{g_{xx}}{g_x}. \tag{5}$$

The modulus of the matrix element of the H_{xx} operator in Eq. (3) is identical to that of the long-range e-h exchange interaction operator calculated in Ref. 15. Based on these earlier calculations, U_{xx} is approximately 1 meV. Further, assuming $2E_g\sim 1$ eV, we obtain that $U_{xx}/2E_g$ is on the order of 10^{-3}. Despite a small value of $U_{xx}/2E_g$, f can still be a significant fraction of unity because of large magnitudes of the factors associated with the matrix elements of optical transitions $V_{\mathrm{intra}}/V_{\mathrm{inter}}$ and the spectral densities of biexciton and single-exciton states $[(g'_{xx})^2(g_{xx}/g_x)]$. Specifically, the ratio between the strengths of intra- and interband transitions in NCs scales as $(R/a_0)^2$ (R is the NC radius and a_0 is the lattice constant) and, therefore, can be much greater than unity, particularly for NCs of large sizes (the R^2 scaling holds until NCs can still be considered as 0D systems, i.e., R^{-1} is comparable or greater than the change in the k vector during the intraband transition).

Further increase in f occurs because of the contribution from multiple intermediate biexciton states. To estimate the number of these states, g'_{xx}, we take into account that they are generated from the vacuum state by the even operator H_{xx} and, therefore, are also even. Upon application to the intermediate $|x_1'x_2'\rangle$ state, the operator H_{ev}^{intra} modifies the quantum state of only one of the four carriers. Therefore, g'_{xx} is the sum of the numbers of possible intermediate states for each of these carriers and it depends on the orbital angular momenta and the projections of the total angular momentum of the carriers in the final state. Depending on a concrete configuration of the final biexciton, g'_{xx} varies from 8 to 16.

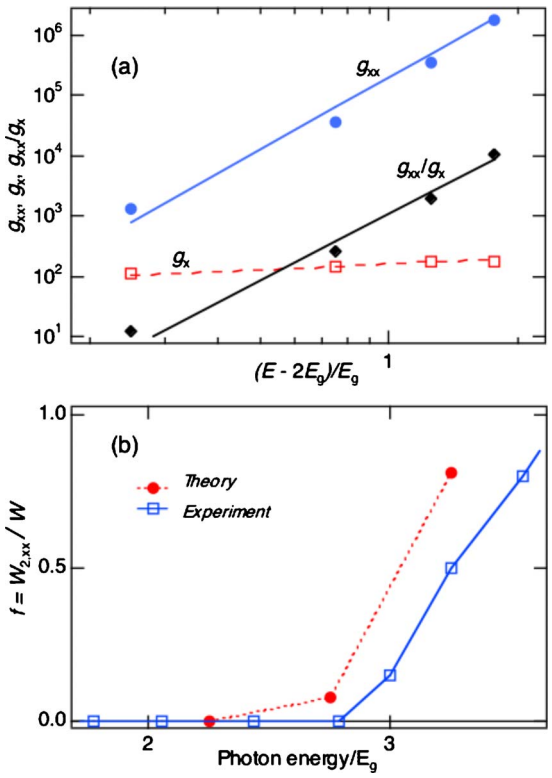

FIG. 3. (Color online) (a) Calculated degeneracy factors for four low-energy $1l$ biexcitons (solid circles) and corresponding near-resonant single-exciton states (open squares) along with their ratio (solid diamonds) shown as a function of energy in access of $2E_g$. Solid lines are fits to $(E-2E_g)^m$, with $m=4$ (g_{xx}) and 3.7 (g_{xx}/g_x); the dashed line is a guide for the eye. (b) Comparison of calculated (solid circles) and measured (open squares; from Ref. 6) values of $f=W_{2,xx}/W$.

Another important factor that increases the value of f is a large number of final biexciton states that can greatly exceed the number of single-exciton states of the same energy. For example, the lowest-energy odd biexciton allowed in the CM process can be in one of two configurations: $|1S(e)1P(h);1S(e)1S(h)\rangle$ or $|1P(e)1S(h);1S(e)1S(h)\rangle$ ($1S1S1S1P$ biexciton). If we account for the $2(2l+1)$-fold degeneracy of electronic states in a single valley and the four-valley character of energy bands, the total number of degenerate biexciton states at the CM threshold is computed to be 1344. A single-exciton state that is near resonance with the $1S1S1S1P$ biexciton has the $|1F(e)1F(h)\rangle$ configuration. The corresponding number of single-exciton resonances for linearly polarized light is 104. Therefore, already at the CM threshold, g_{xx} exceeds g_x by more than a factor of 10.

The g_{xx}/g_x ratio rapidly increases with energy [approximately as $(E-2E_g)^{3.7}$], as illustrated in Fig. 3(a) for biexcitons with the configuration $|1l_1(e)1l_2(h);1l_3(e)1l_4(h)\rangle$ ($1l$ biexcitons). The degeneracy of these biexcitons is particularly high [scales with E as $(E-2E_g)^4$, Fig. 3(a)] because the electron and hole $1l$ states are nearly equidistant[5,15] and, further, because the spacing between these states is nearly identical in both the valence and the conduction bands. By taking into account various sources of degeneracy, we calculate that

g_{xx}/g_x is ~250, ~2000, and ~10^4 for the second ($E_{xx}=2.75E_g$), the third ($3.25E_g$), and the fourth ($3.75E_g$) $1l$ biexciton states allowed in the CM process, respectively.

Using these values, we further obtain that f is on the order of a fraction of a percent ($f=0.002$) at the CM threshold (estimated for $R\sim 3$ nm). However, because of the rapid increase in the g_{xx}/g_x ratio with energy, f is 0.08 for $E_{xx}=2.75E_g$ and ~0.8 for $E_{xx}=3.25E_g$. The overall spectral dependence of calculated values is consistent with CM efficiencies observed experimentally for PbSe NCs [Fig. 3(b)].

V. VIRTUAL EXCITON VERSUS VIRTUAL BIEXCITON PATHWAY

Using second-order perturbation theory, we can estimate the relative CM efficiencies for the virtual exciton and the virtual biexciton channels. Specifically, we can obtain the following approximate expression for the ratio of the $W_{2,xx}$-to-$W_{2,x}$ rates for the case when both pathways lead to the same final biexciton state:

$$\frac{W_{2,xx}}{W_{2,x}} \approx \left(\frac{g'_{xx}}{g'_x}\frac{V_{\text{intra}}}{V_{\text{inter}}}\frac{U_{xx}}{U_{II}}\right)^2 \frac{\Delta_x^2+\Gamma^2}{4E_g^2}, \tag{6}$$

where g'_x is the number of intermediate single-exciton states, Δ_x is the average detuning of an incident photon from the virtual single-exciton transition, and Γ is this transition linewidth.

According to calculations of Ref. 10, the unscreened value of U_{II} for PbSe NCs of $R\sim 3$ nm radius is ~20 meV, which translates into the screened interaction energy of ~1 meV (estimated using a high-frequency permittivity of PbSe of 23). The latter value is comparable to the e-h exchange interaction energy calculated in Ref. 15, which implies that $U_{xx}/U_{\text{II}}\sim 1$. Under the resonant condition for the virtual exciton pathway, we can neglect Δ_x compared to Γ. If we further disregard nonresonant transitions, we can assume that $g'_x=2$, while g'_{xx} is approximately 10. Finally, assuming $V_{\text{intra}}/V_{\text{inter}}\approx 5$, we obtain $W_{2,xx}/W_{2,x}\approx(25\Gamma/2E_g)^2$. Even in the case of highly monodisperse NC samples, the transition broadening is dominated by distribution in NC sizes, which results in the ensemble linewidth of ~100 meV. Using this value, we obtain that for $2E_g$ of 1 eV, $W_{2,xx}/W_{2,x}\approx 6$. This result shows that the efficiency of the CM channel mediated by intraband transitions is comparable to or greater than the efficiency of the impact-ionization-like process mediated by interband transitions even in the case when the latter is estimated for favorable resonant conditions.

VI. CARRIER MULTIPLICATION AND OPTICAL ABSORPTION

An interesting question is whether CM by direct photogeneration of multiexcitons leads to increased optical absorption of the sample. This issue was analyzed in Ref. 10 for the case of interband excitation of intermediate exciton states. Specifically, it was shown that Coulomb coupling between single- and biexciton states does not increase overall (spectrally integrated) interband optical absorption. Therefore,

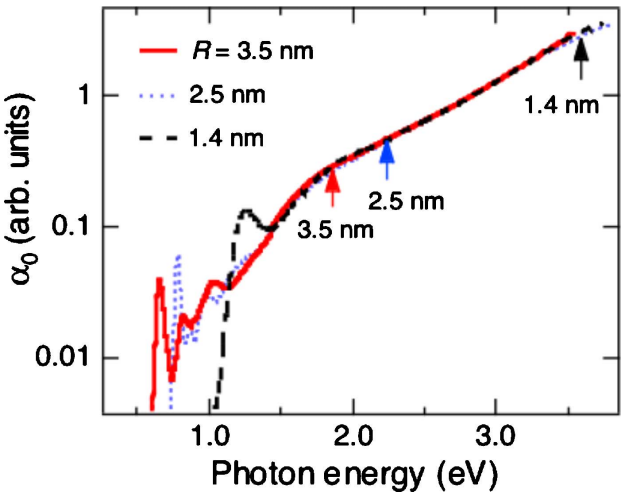

FIG. 4. (Color online) Spectral dependence of the absorption coefficient (α_0) of PbSe NCs of three different mean radii (indicated in the figure). Arrows show the onset for CM calculated from $\hbar\omega_{\text{CM}}=2.85E_g$.

CM for the virtual exciton channel can be interpreted in terms of redistribution of the oscillator strength between single-exciton and biexciton resonances (biexcitons "borrow" oscillator strength from single excitons). Direct generation of biexcitons via the virtual biexciton channel is also accompanied by reduction of single-exciton absorption. In this case, the reduction is a result of partial depletion of the valence band population, which occurs as a consequence of excitation of virtual biexcitons by the Coulomb interaction.

While not changing overall absorption, the CM process can lead to spectral changes in the absorption coefficient (manifested, e.g., in the shift of existing lines and the development of "biexcitonic" absorption features). However, since Coulomb energies are expected to be small compared to transition linewidths, the spectral modifications associated with CM are likely insignificant and not readily detectable experimentally. For example, as evident from Fig. 4, the absorption spectra of PbSe NCs of different sizes (i.e., different band gaps) closely match each other at high spectral energies despite the difference in the CM thresholds (positions of $\hbar\omega_{\text{CM}}$ for different samples are shown in Fig. 4 by arrows) and, hence, independent of whether photon absorption produces single excitons or multiexcitons.

VII. CONCLUSIONS

In conclusion, we propose and analyze a mechanism for direct photogeneration of biexcitons in NCs, which involves excitation of a virtual biexciton from NC vacuum by the Coulomb interaction between two valence-band electrons, followed by the conversion of the virtual biexciton into a real biexciton by absorption of a photon on an intraband optical transition. This mechanism is not active in bulk materials because of momentum conservation, which suppresses virtual intraband transitions. On the other hand, because of relaxation of momentum conservation, the proposed mecha-

nism becomes highly efficient in 0D structures providing a significant contribution to CM in NCs. Specifically, our estimates indicate that the biexciton generation rate for the process mediated by intraband optical transitions is comparable to or even greater than that for the impact-ionization-like pathway due to interband transitions. Since relaxation of translational-momentum conservation is a general feature of low-dimensional semiconductors, the CM mechanism mediated by intraband optical absorption can be highly efficient not only in 0D NCs but also in other types of quantum-confined nanostructures.

ACKNOWLEDGMENTS

This work was supported by the Chemical Sciences, Biosciences, and Geosciences Division of the Office of Basic Energy Sciences, Office of Science, U.S. Department of Energy and Los Alamos LDRD funds. V.I.K. acknowledges support by the Center for Integrated Nanotechnologies (CINT), a U.S. Department of Energy, Office of Basic Energy Sciences, nanoscale science research center operated jointly by Los Alamos and Sandia National Laboratories.

*valery_rupasov@hotmail.com
†klimov@lanl.gov

[1] P. T. Landsberg, *Recombination in Semiconductors* (Cambridge University Press, Cambridge, 1991).
[2] C. A. Klein, J. Appl. Phys. **39**, 2029 (1968).
[3] R. C. Alig and S. Bloom, Phys. Rev. Lett. **35**, 1522 (1975).
[4] R. D. Schaller and V. I. Klimov, Phys. Rev. Lett. **92**, 186601 (2004).
[5] R. Ellingson, M. C. Beard, J. C. Johnson, P. Yu, O. I. Micic, A. J. Nozik, A. Shabaev, and Al. L. Efros, Nano Lett. **5**, 865 (2005).
[6] R. D. Schaller, M. Sykora, J. M. Pietryga, and V. I. Klimov, Nano Lett. **6**, 424 (2006).
[7] M. Califano, A. Zunger, and A. Franceschetti, Appl. Phys. Lett. **84**, 2409 (2004).
[8] A. Franceschetti, J. M. An, and A. Zunger, Nano Lett. **6**, 2191 (2006).
[9] G. Allan and C. Delerue, Phys. Rev. B **73**, 205423 (2006).
[10] A. Shabaev, Al. L. Efros, and A. J. Nozik, Nano Lett. **6**, 2856 (2006).
[11] R. D. Schaller, V. M. Agranovich, and V. I. Klimov, Nat. Phys. **1**, 189 (2005).
[12] V. B. Berestetskii, E. M. Lifshits, and L. P. Pitaevskii, *Quantum Electrodynamics* (Elsevier, Oxford, 1981).
[13] A. Smith and D. Dutton, J. Opt. Soc. Am. **48**, 1007 (1958).
[14] P. Guyot-Sionnest and M. A. Hines, Appl. Phys. Lett. **72**, 686 (1998).
[15] I. Kang and F. W. Wise, J. Opt. Soc. Am. B **14**, 1632 (1997).